Boronated Compounds for Imaging Guided BNCT Applications.

(Article begins on next page)

26 April 2024

Boronated Compounds for Imaging Guided BNCT Applications

Simonetta Geninatti-Crich, Annamaria Deagostino, Antonio Toppino, Diego Alberti, Paolo Venturello, Silvio Aime

a Dipartimento di Chimica Generale e Chimica Organica, Università degli studi di Torino, Via Pietro Giuria, 7, 10125 Torino, Italy.
Fax: +390116707642; Tel: +390116707647; E-mail: annamaria.deagostino@unito.it
b Dipartimento di Chimica IFM, Università degli Studi di Torino, Via Pietro Giuria, 7, 10125 Torino, Italy.

Abstract

Boron neutron capture therapy (BNCT) is based on the capture of thermal neutrons by boron 10 (^{10}B) nuclei that have been selectively delivered to tumor cells. The amount of 10-30 µg of boron for g of tumor mass is needed to attain an acceptable therapeutic advantage. Despite the potentialities of BNCT have been demonstrated in several preclinical studies, this technique has not yet been fully accepted in the armoury of tools for tumor treatment. This is partly due to the differences in the uptake and distribution of ^{10}B among patients and also to the uncertainty found in the determination of tumor-to-blood ^{10}B concentration ratio. Attention is now being payed to use the main imaging techniques to determine the *in vivo* biodistribution of BNCT agents. Most of the work has been devoted to the most promising BNCT agents, namely BPA, BSH and carborane derivatives. This review surveys studies carried out over the last decade, and outlines the role that NMR, PET and SPECT imaging may have to improve the efficacy of BNCT.

Keywords: biodistribution, BNCT, ^{10}B NMR, imaging, ^{11}B NMR, BPA, BSH, carboranes, ^{19}F NMR, ^{1}H-MRI, ^{1}H-MRS, PET, SPECT, therapy, tumors.

Introduction

Boron neutron capture therapy (BNCT) is a type of binary radiation therapy currently under intense scrutiny for the treatment of cancer, especially of malignant brain tumors. It is based on the capture of thermal neutrons by boron 10 (^{10}B) nuclei that have been selectively delivered to tumor cells. The neutron capture event results in the formation of excited ^{11}B nuclei that undergo fission to yield highly energetic ^{4}He^{2+} and ^{7}Li^{3+} ions. Cell death is triggered

1

by the release of these charged particles which create ionisation tracks along their trajectories, resulting in cellular damage. Both the alpha particle and the lithium ion produce closely spaced ionizations in the immediate vicinity of the reaction, with a range of approximately 5-9 micrometres, or roughly the thickness of one cell diameter. It has been estimated that approximately 10-30 µg of ^{10}B for g of tumor mass is needed to attain an acceptable therapeutic advantage.[1, 2]

Many preclinical studies have shown the potential of BNCT in the treatment of many tumors such as malignant glioma,[3, 4] melanoma,[5, 6] metastatic disease in the liver,[7, 8] head and neck tumors,[9, 10] and thyroid carcinoma,[11, 12] which are tumors characterized by high mortality and very poor life expectancy.

Currently, two BNCT drugs are available for clinical investigation (Figure 1):

L-*para*-Boronophenylalanine (**BPA**, $C_9H_{12}{}^{10}BNO_4$) which is structurally correlated to the neutral amino acid phenylalanine and has been used in clinical trials to treat glioblastoma and melanoma.[13]

Sodium mercaptoundecahydro-*closo*-dodecaborate (**BSH**, $Na_2{}^{10}B_{12}H_{11}SH$) which is a derivative designed for brain tumor treatment. It has been investigated in the treatment of malignant glioma and in a phase-I trails for glioblastoma multiforme (EORTC) 119610.[14]
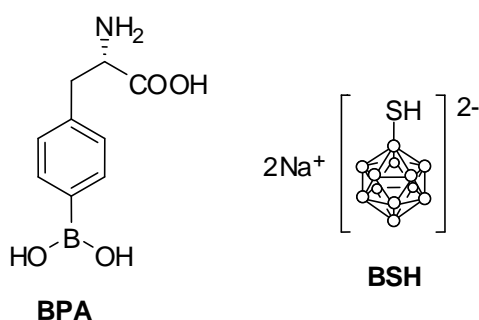

Figure 1 BPA and BSH structures

The first clinical use of BSH was reported by H. Hatanaka in the 1960s for the BNCT of patients with high grade gliomas,[15] and BPA was first used clinically by Mishima in 1988-9 to treat patients with cutaneous malignant melanomas.[16]

Currently, the BPA-fructose complex, which displays an improved water solubility in comparison to BPA, is the most frequently used clinical boron agent for both intra- and extra-cranial tumors.[17] Recently, BSH has been administrated intravenously either alone, or in combination with BPA.[18, 19]

Despite their clinical use, both BPA and BSH show low selectivity and great efforts have been made by several research groups to develop new and more selective boron delivery agents. Polynuclear boron derivatives have been considered potential candidates for BNCT applications and several readily functionalized carboranes have been used to design boron delivery vehicles for BNCT because of their high boron content and their *in vivo* stability.[20-22]

The use of NCT to destroy diseased cells was proposed a long time ago.[23] In spite of huge potential, it has not attained an established position in the armory of anti tumor therapies. However, the methodology has never been discarded and it remains in a sort of "limbo" with some enthusiastic supporters and many critical spectators (usually partisans of other therapeutic

2

modalities). In fact, one of the most attractive characteristics of this technique is that if the [10]B can be selectively delivered to tumor cells, the short range of the high LET charged particles offers the potential to selectively irradiate individual tumor cells causing little or no effect on normal cells and tissues adjacent to the tumor.[24] A crucial issue is the assessment of the amount of boron-10 that has reached the target sites. This is important in order to proceed with the neutron irradiation step because successful results can only be expected if the boron concentration threshold has been reached. Moreover to fully understand the impact and the feasibility of BNCT therapy, it is important to evaluate the transport and the exchange dynamics of boron in a variety of biological samples.

This could not be accomplished without an imaging agent coupled with the BNCT compound. This review is devoted to survey studies where the main imaging techniques have been applied to BNCT over the last decade. In particular, the applications of NMR, (MRS and MRI) and PET techniques in the evaluation of the biodistribution and kinetics of boron derivatives in preclinical and clinical studies will be reported. NMR detection of BNCT molecules has been pursued either by the spectroscopic (MRS) and the imaging (MRI) modalities. The nuclei that have been considered are ^{1}H, ^{19}F and ^{10}B/^{11}B.

^{19}F NMR detection

Some of the current applications of ^{19}F NMR imaging and spectroscopy in living systems were suggested in the 1970s, at the time of the first human ^{1}H MRI applications. The ^{19}F nucleus has a 100% abundance, resonates at a resonance frequency that is 94% that of ^{1}H and its NMR sensitivity is 83% that of a ^{1}H (with constant noise), so that the signal to noise ratio (SNR) expected in ^{19}F MR images is about 89% that of ^{1}H per nucleus, assuming sample-dominant noise. There is a negligible endogeneous ^{19}F MRI signal from the body, as the physiological concentration of detectable mobile fluorine is below the detection limit (usually less than 10^{-3} μmol/g wet tissue weight). Fluorine exists at higher concentrations in the bone matrix and teeth, but, being immobilized, exhibits a very short spin-spin relaxation (T_2) which is not visible by conventional MRI methods. This lack of background signal provides ^{19}F MRI with a potentially very high contrast-to-noise ratio and specificity, if a fluorinated compound can be introduced as a contrast agent.[25]

Some examples of the synthesis of molecules which contain both ^{10}B and ^{19}F atoms have been reported by Hattori and researchers. In a recent paper they described the synthesis[26] of β-[4-(^{10}B)borono-2,6-difluorophenyl]alanine (R = COOH) and of β-[4-(^{10}B)borono-2,6-difluorophenyl]alaninol (R = CH$_2$OH) (Scheme 1).

3
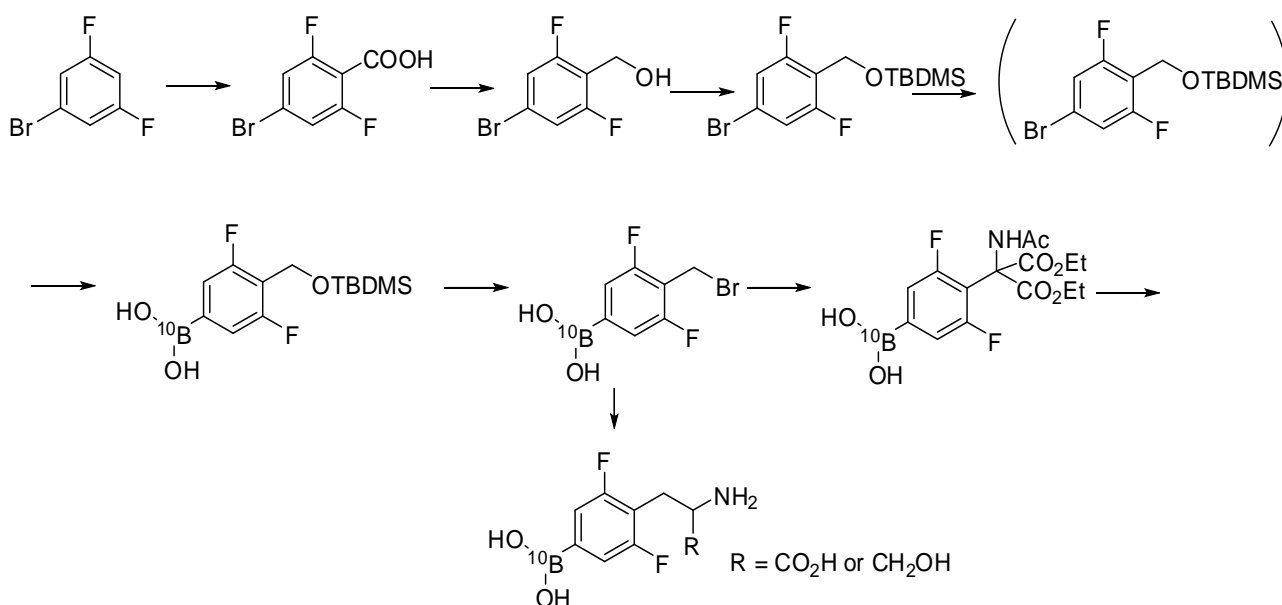
Scheme 1 Synthesis of β-[4-(^{10}B)borono-2,6-difluorophenyl]alanine (R = COOH) or β-[4-(^{10}B)borono-2,6-difluorophenyl]alaninol (R = CH$_2$OH).

Cellular uptake and cytoxicity of the two BPA derivatives have been investigated using C6 (rat glioma), HeLa (human epithelioma) and KB (human squamous cell carcinoma) cells. In C6 cells, the amount of both β-[4-(^{10}B)borono-2,6-difluorophenyl]alanine and β-[4-(^{10}B)borono-2,6-difluorophenyl]alaninol was half that of BPA, whereas in KB and HeLa cells the amounts of internalized compound was the same as BPA. Moreover no citotoxicity of these compounds toward C6 cells was observed in the 1 – 20 mM concentration range. The same group designed and synthetized ^{10}B BPA derivatives containing the trifluoromethyl group.[27] In order to use these compounds in ^{19}F MRI, the detection-sensitivity in their ^{19}F NMR measurement in deuterium saline was determined. As expected, the results showed that the signals of trifluoromethylated derivatives are much more easily detected that those ones afforded by the difluorinated derivatives. The fluorinated compounds were then incorporated into Ihara cells. The results clearly demonstrated that all the synthetized fluorinated derivatives were usable as ^{19}F probes, the carboxylic derivatives being more sensitive than the corresponding alcohol derivatives. The tumor killing ability of these compounds was then evaluated in BNCT applications.[28]

Recently, studies dealing with the potential use of L-DOPA as an enhancer of BPA accumulation in malignant gliomas have been reported.[29-31] The investigation was first carried out *in vitro*, and then extended to *in vivo* C6 glioma animal model. With the aim of evaluating *in vivo* the boron distribution and pharmacokinetics, the study was extended to 4-borono-2-fluorophenylalanine (^{19}F-BPA) where ^{19}F MR imaging and spectroscopy were utilized.[32, 33] The fluorinated derivative was administered as ^{19}F-BPA – fructose complex. The results are reported in Figure 2 . The ^{19}F MRI images indicate an improved ^{19}F-BPA – fructose complex uptake in C6 tumor bearing rats after L-DOPA pretreatment. It should be underlined that both ^{19}F MRS and MRI offer the possibility of following the pharmacokinetics and the visualization of the concentration gradient between the tumor and the normal tissue for these ^{10}B-carrying drugs. A density functional investigation of the complexes of ^{10}B enriched BPA with ß-D-fructofuranose has been recently reported. The BPA-fructose may exists in three forms where the boron atom is differently bonded to oxygen, the

calculations indicate that the abundant oxygen atoms may play an important role in the interaction of BPA-fructose complexes and their envinronment.[34]
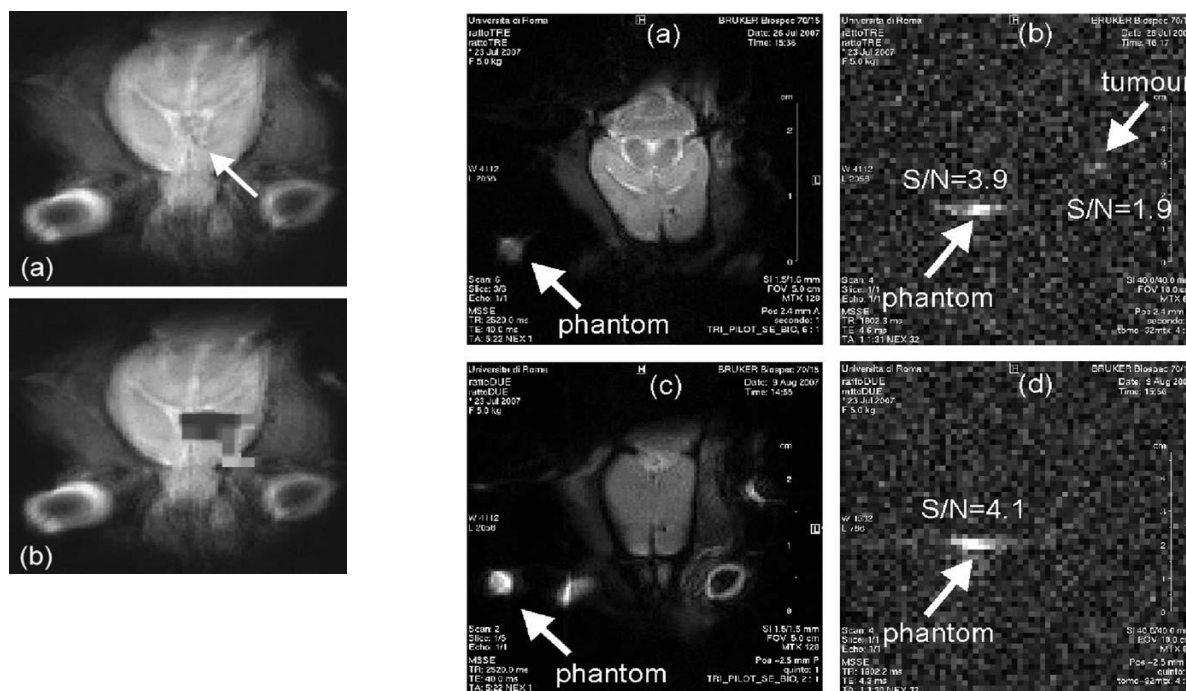

Figure 2 ^{1}H axial image of rat brain by overlapping all proton slices (a, left), superimposition of ^{19}F MRI axial image of rat brain (b, left); [1]H T2-weighted axial reference (a, right), ^{19}F axial image of rat brain preloaded with L- DOPA and infused with ^{19}F-BPA – fr complex (b, right), [1]H T2-weighted axial reference (c, right),[19]F axial image of rat brain not preloaded with L- DOPA but infused with ^{19}F-BPA – fr complex (d, right) (images reprinted with the permission of the editor, license number 2762400037562).

.

[10]B and ^{11}B NMR detection

Boron containing molecules are known not to play a significant natural role in mammalian cells or organs, therefore biomedical applications of [10]B and ^{11}B NMR have been mostly limited to the xenobiotics compounds administrated to the investigated biological systems. The majority of publications deals with molecules that are used as BNCT agents in experimental cancer models. Both natural boron isotopes [11]B (80% natural abundance) and [10]B (20% natural abundance) are detectable by NMR. [11]B has spin 3/2, a quadrupole moment of 4.06 fm^2, and a relative gyromagnetic ratio of 0.32, whereas [10]B has spin 3, a quadrupole moment of 8.46 fm^2, and a relative gyromagnetic ratio of 0.107. In consideration of the natural abundance and the nuclear properties, [11]B displays a higher sensitivity and better spectral resolution than [10]B. However, the peculiar relaxation properties of spin 3 nuclei cause the [10]B T_2 to be longer than [11]B T_2 for the same molecular site that can constitute a significant detection advantage for [10]B. However, both the boron isotopes have been investigated in MRI-BNCT applications.

In 2001 Bendel and coworkers published the first *in vivo* MRI images of [10]B enriched BSH.[35] BSH was injected into the tail vein of mice with implanted M2R melanoma xenografs and was imaged

using 3D gradient echo ^{10}B MRI. The ^{10}B images were compared with ^{1}H images, as showed in Figure 3 . It was also demonstrated how the shorter T_1 value of ^{10}B, compared to ^{1}H, could be an advantage for the direct BSH ^{10}B MRI detection. Moreover it was demonstrated that *in vivo* MRI detection of ^{10}B enriched BSH at realistic tissue concentration levels, with an acceptable spatial resolution and in reasonable imaging times was possible.
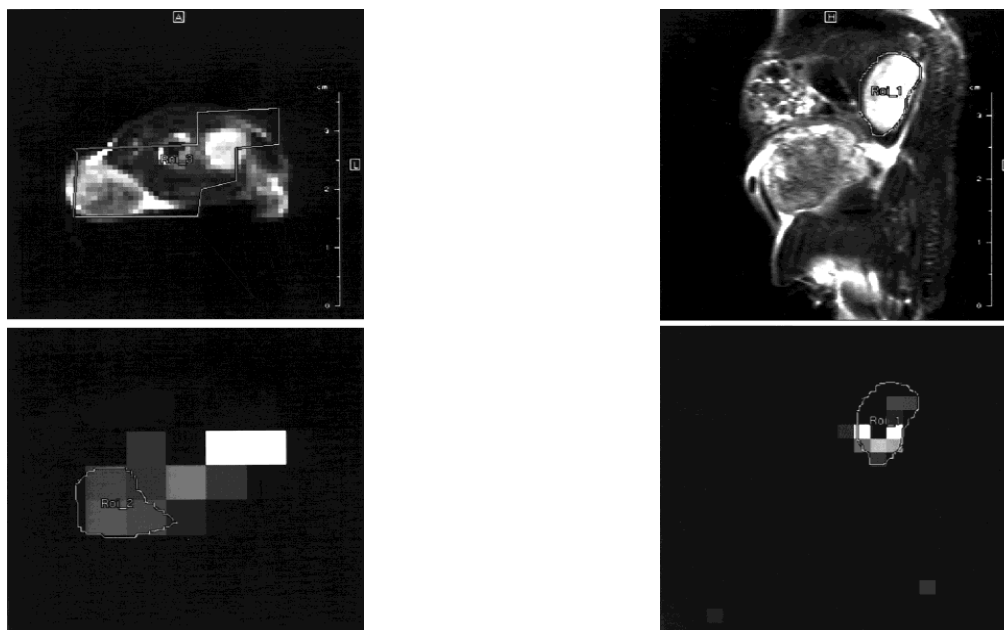

Figure 3 ^{1}H (left, top) and ^{10}B (left, bottom) images at a corresponding slice locations through a mouse with implanted tumor; ^{1}H (right, top) and ^{10}B (right, bottom) images acquired using a "high resolution protocol" at a corresponding slice locations through another mouse with implanted tumor (images reprinted with the permission of the editor, license number 2762950831156)

^{11}B NMR was used by the same research group to evaluate the differences in the retention of boromercaptate monomer (BSH) and the corresponding dimer (BSSB) in malignant cells.[36] ^{11}B NMR at sufficiently high magnetic fields is able to distinguish between boron in different molecules, e. g. between BSH and BSSB. This study confirmed that the uptake of BSSB in M2R melanoma and C6 rat glioma cells was not significantly different from that of BSH. Furthermore, since differences became apparent only a long time after infusion, the authors surmised that they were caused by differences in the retention, rather than in the uptake stage. They also proposed the use of BSSB as a BNCT agent. Time-dependent metabolic changes in BSH and BPA-fructose complexes were also studied using the ^{10}B NMR analysis of human urine samples periodically collected from head and neck squamous cell carcinoma patients.[37] It was observed that, on one hand, the BPA – fructose complex dissociated producing the corresponding constituents BPA and fructose, and that the borate group was partly cleaved from BPA. On the other hand, BSH was partly aggregated to a dimer form, as it has previously been reported for cultured cells and animal models and confirmed in human cancer patients in this study.

^{1}H-MRI
^{1}H- Magnetic Resonance Imaging (MRI) has been proposed to assess the biodistribution of BNCT compounds. Although its sensitivity its lower in comparison to nuclear and optical modalities, the high spatial resolution (<100um) of ^{1}H-MRI can provide detailed morphological and functional information, and the absence of radiation makes it more safe than techniques based on the use of

radioisotopes.[38] MRI signal is dependent on the longitudinal (T_1) and transverse (T_2) proton relaxation times of water and therefore the contrast in a MR image arises mainly from differences in the relaxation times of tissue water protons as a consequence of the interaction with biological macromolecules and membranes. In both clinical and experimental settings the endogenous contrast can be altered by the use of contrast agents (CA) that decrease the longitudinal and transverse relaxation time of water protons in the tissues were they distribute.[39, 40] Most of the contrast agents used in clinical settings are polyaminocarboxylate complexes of Gd^{3+} ion that contains seven unpaired electrons. The ligands are multidentate (seven or eight donor atoms) in order to form complexes with very high thermodynamic and kinetic stability thus limiting the release of the free metal ion that are highly toxic because they interfere with Ca^{2+} pathways. The coordination cage of the Gd^{3+} ion is completed with 1 or 2 water molecules that are responsible for transferring, through a fast chemical exchange, the paramagnetic properties to the overall bulk water molecules. The ability of a Gd^{3+} chelate to affect the water proton relaxation times is represented by the relaxivity value (i.e. the relaxation enhancement of solvent water protons in the presence of 1 mM concentration of the paramagnetic agent). In a proton MR image there is a direct proportionality between the observed relaxation enhancement and the concentration of the paramagnetic MRI reporter. Thus these agents can be used to carry out an indirect Boron quantification upon their linking to the neutron capture compound. Interestingly, a given cell can be visualized by MRI when the number of Gd^{3+} complexes is of the order of 10^8-10^9 per cell, i.e. a threshold close to that found for the number of ^{10}B atoms necessary to provide an effective NCT treatment.[41]

Different types of dual probes, containing both a paramagnetic ion for MRI detection and ^{10}B atoms for BNCT, have been reported in the last ten years (Figure 4). Yamamoto and coworkers synthesized two Gd-DTPA complexes functionalized with a carborane and a BPA unit,[42-44] respectively. The latter compound (Figure 4) showed higher accumulation in tumor cells with respect to the former. However, the conjugation of a Gd-DTPA unit (MW= 590 Da, two negative charges) to BPA (MW=209 Da, neutral at pH=7) causes a dramatic change in the biodistribution and the intratumor boron concentration of BPA-Gd-DTPA was significantly reduced with respect to BPA alone as a consequence of the decreased affinity of BPA-Gd-DTPA for BPA receptors or as a consequence of a change in the internalization pathway.
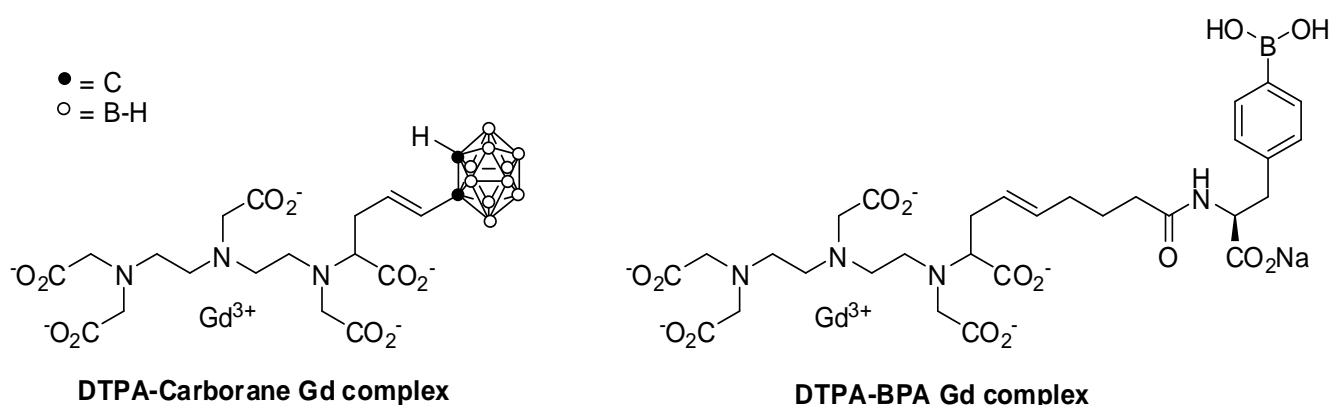

DTPA-Carborane Gd complex

DTPA-BPA Gd complex

Figure 4 DTPA-Carborane and DTPA-BPA Gd complexes

Using nanosized carriers (i.e. liposomes, micelles, polymers, proteins etc.), it is possible to deliver, at the same time both NC and MRI contrast agents without any alteration of their biodistribution. Recently, we reported the use of a dual MRI/BNCT probe,[45, 46] containing a carborane unit (with 10 boron atoms) linked to a Gd-DOTA monoamide complex for MRI and to an aliphatic chain (C15) (**AT101**, Figure 5) for the binding to a biological nanocarrier represented by Low Density Lipoproteins (LDL).
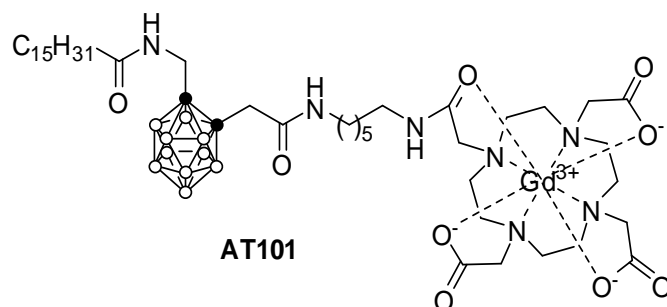

Figure 5 Structure of AT101

LDLs have been identified as good candidates in carrying boron to tumor cells since the expression of their receptors is upregulated in many types of tumor cells. LDLs provide cholesterol for the synthesis of the membranes in fast proliferating cells. The amount of Gd and B atoms taken up by the cells was determined by ICP-MS analysis (Figure 6A). The B/Gd molar ratio found in tumor cells (hepatoma, melanoma, glioma cells) was consistently about 10:1, thus indicating the absence of Gd/B/L degradation or release of Gd upon incubation. The lowest boron concentration that can be detected *in vivo* using proton MRI is 1 ppm that corresponds to the minimal detectable variation of the signal intensity measured in the region of interest (Figure 6B,C). BNCT was performed inside the thermal column of the TRIGA Mark II reactor at the University of Pavia on B16 melanoma tumor bearing mice 6 h after the administration of the B/Gd agent. At that time an intratumor boron concentration of more than 30 ppm was measured by MRI. BNCT treatment resulted in a dramatic reduction in tumor growth over that observed in untreated animals.
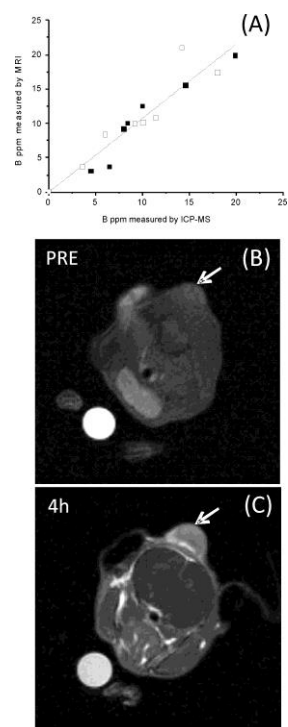
Figure 6 (A) Correlation between intracellular Boron concentrations measured by ICP-MS and MRI. Boron concentrations were measured in B16 murine melanoma cells (■) and HepG2 Human hepacoarcinoma cells (□) after 16h of incubation at different Gd-B-L/LDL particle concentrations. (B,C) Representative T_1-weighted MR images of C57BL/6 mice grafted subcutaneously with B16 melanoma cells acquired before (B) and 4 (C) hours after the administration of Gd-B-L/LDL particles. The arrows indicate tumor regions.

It must be underlined that Gadolinium has been recently proposed, as neutron capture agent in NCT, due to the nuclide high neutron capture cross section (254000 b for ^{157}Gd vs 3835 b for ^{10}B). Gadolinium neutron capture reactions release a wide range of particles: prompt gamma rays, internal conversion electrons, X-rays and Auger electrons. The presence of strong gamma rays spreads out the dose delivery to a broad region, thus limiting the selectivity of the therapy. The photons emitted in the (n,γ) reactions interact with the tissues but deposit energy over a longer path length than the boron reaction products. This is the main drawback of GdNCT.[42]

Another example of a dual MRI/BNCT probe can be seen in Boron nitride nanotubes (BNNTs) that are nanostructured compounds with a graphite-like sheet structure made of alternating B and N atoms.[47] They have recently been proposed as BNCT agents which are able to introduce high boron concentration in neoplastic cells.[48] The presence of paramagnetic iron impurities also renders these materials suitable as MRI negative (T2) contrast agents.[49] Indeed, the performance of Fe-containing BNNTs as contrast agents has already been assessed by determining the longitudinal (r1) and transverse (r2) water proton relaxivities of BNNT aqueous dispersions at 1.5, 3 and 7.05 T. The T2-weighted images of BNNT dispersions at different concentrations recorded at 3 T showed significant signal attenuation as the concentration increased from 0 to 300 mg [BNNT]/ml, confirming the potential of these materials as negative contrast agents.[50]

^{1}H-MRS

Proton magnetic resonance spectroscopy (^{1}H-MRS) allows the non-invasive *in vivo* detection and quantification of metabolites.[51] It has been proposed as a non-invasive method to evaluate boron concentration *in vivo* upon BPA administration. The BPA detecting and quantifying capabilities of

9

various MRS and spectroscopic imaging (^{1}H MRSI) methods have been investigated over the last ten years.[35, 52-54] *In vivo* ^{1}H MRS detection of BPA is based on its aromatic protons. In fact, the aromatic proton chemical shift region (6.5–9.0 ppm) of the human brain usually contains only weak brain metabolite and macromolecule signals, therefore, the aromatic proton signals of BPA (four signals centered at ~7.4 ppm) appear to be easily detectable and privy of interfering peaks (Figure 7).[55]
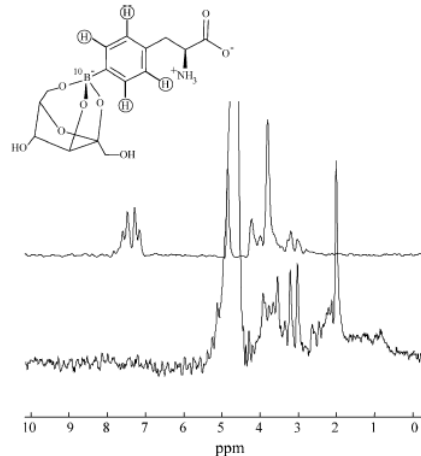

Figure 7 The 1.5 T white matter ^{1}H spectrum of a healthy volunteer (lower) and a phantom spectrum obtained from a BPA-F solution (upper) using TE of 30 mS (images reprinted with the permission of the editor, license number 2762500767890).

The possibility of detecting the aromatic BPA protons has previously been recognized and demonstrated on a patient using standard STEAM (Stimulated Echo Acquisition Mode, TE=30ms).[56] Afterwards modified methods were introduced in order to increase the efficiency for such detection.[57] Bendel and coworkers performed MRSI of BPA biodistribution in a mouse kidney (Figure 8) by introducing, along with the spatially selective pulses, a chemical shift selective pulse focused on the spectral region of the aromatic BPA protons.[58]
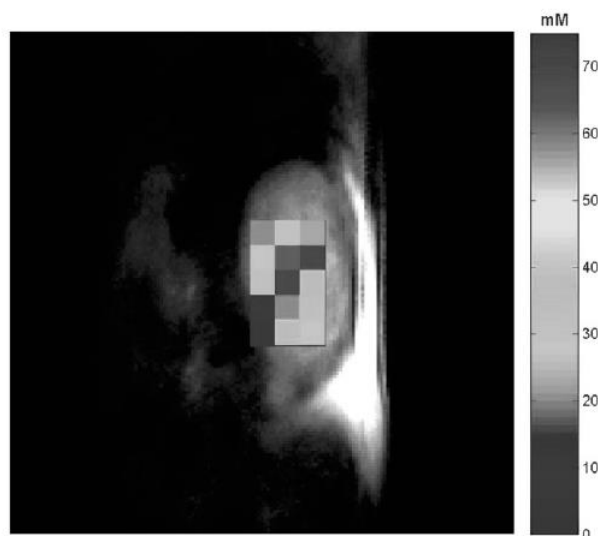

10

Figure 8 BPA concentration map derived from dividing the BPA from the water intensity map superimposed on the FSE kidney image (images reprinted with the permission of the editor, license number 2762501109022).

The detection limits of BPA at 1.5 and 3.0 T have been determined *in vitro* to be 1.4 mM (1.5 T) and 0.7 mM (3.0 T), respectively, using a typical clinical voxel size of 8 ml and a clinically compatible ^{1}H MRS measurement time of ~10 min. Based on these results, it was estimated that the *in vivo* detection limit at 1.5 T was approximately 2 mM BPA (~20 mg/kg of ^{10}B in the brain). BNCT is frequently applied after the surgical removal of malignant glioma. The remaining residual tumor forms a narrow lining in the wall of the resection cavity which contains haemostatic agents and coagulated blood with fluid-tissue and fluid-air interfaces. This could be a problem because the voxel contains resected areas that generate interference in the ^{1}H-MRS detection of BPA.[59] For this reason un-operated tumors are more suitable for MRS based BPA detection. One may conclude that the main advantage of ^{1}H-MRS is that it allows BPA concentrations in the tumor tissue to be assessed during the intravenous infusion of the boron carrier and that, whereas direct ^{10}B NMR detection needs additional nonstandard hardware, the technique is available in the majority of high field clinical MRI scanners. The disadvantage is the low sensitivity that needs to be improved.

PET detection

Radiolabeled derivatives are of particular interest for *in vivo* imaging of boron compounds, since their biodistribution can be easily monitored by using SPECT (single-photon emission computed tomography) and PET (positron emission tomography), depending on the radionuclide employed. In PET imaging, positrons are emitted by the radionuclide and they interact with a negatron (electron) in an annihilation process. This process produces two coincident 511 KeV photons, which are detected simultaneously in a detector ring.[60] The introduction of PET has represented a significant advance in cancer imaging and has improved the management of patients. During the last decade several PET radiopharmaceuticals entered the clinic and PET became an important tool for the staging of cancer patients and assessing response to therapy. The physical integration of PET and computed tomography (CT) in hybrid PET/CT scanners allows a combined anatomical and functional imaging. PET can be used for tumor staging, for prediction of tumor response to the therapy, for the detection of early recurrence, and for monitoring the therapeutic treatment. When a PET tracer is coupled to a BNCT agent it yields another route for the localization and quantification of the BNCT agent before and after the therapeutic treatment.

The first in vivo study of pharmacokinetics and quantification of a BNCT agent was performed by Kabalka et al in USA,[10, 61] and Imahori et. al. in Japan,[62, 63] using ^{18}F-^{10}B-fluoroboronophenylalanine (^{18}FBPA) as ^{18}F is one of the most common PET isotope.

PET was used to determine the prognostic significance of the metabolic values and ratios of ^{18}FBPA in a study dedicated to evaluating the long term outcomes of gliomas treatment using ^{18}FBPA on 22 patients.[64] In this paper it was shown that the kinetic constants of ^{18}FBPA metabolism are an important factor in the prediction of the prognosis and could be a good biomarker for the feasibility of BNCT with gliomas.

The 4-borono-2-[^{18}F]-fluoro-L-phenylalanine-fructose complex (^{18}FBPA-fr) injected in brain rats with F98 glioma was investigated by *in vivo* small PET imaging (high resolution microPET).[65, 66]
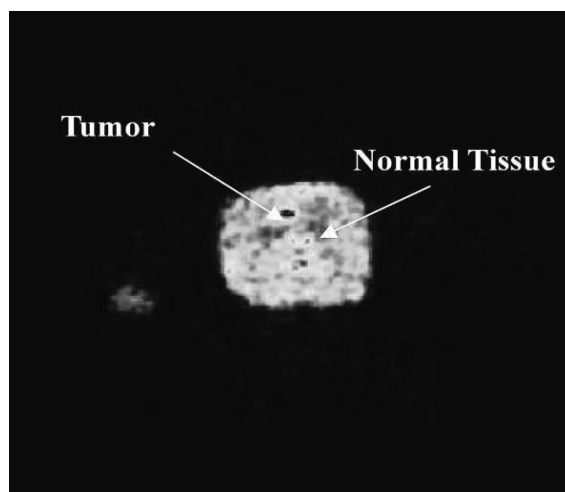

Figure 9 The 27th tomographic slice of microPET images of a F98 glioma-bearing Fischer 344 rat at the 15th time frame after intravenous injection of 20 M Bq (^{18}FBFA-fr), (images reprinted with the permission of the editor, license number 2762420665218).
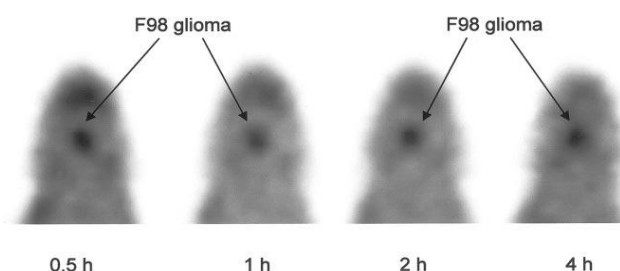

Figure 10 PET images of F98 glioma-bearing Fischer 344 rat at 0.5, 1, 2 and 4 h after intraveneous injection of 20.35 MBq (^{18}FBFA-fr) (images reprinted with the permission of the editor, reference number RQ01334).

The study was applied to 344 rats. The images (see Figure 9 and Figure 10) showed a tumor-to-normal uptake ratio of ~3:1. The microPET imaging used with ^{18}FBPA-fr complex demonstrated to be a suitable probe for ^{18}F^{10}BPA -fr detection in BNCT. Also in this case it was demonstrated that the tracer uptake capacity, associated with tumor malignancy, depended on the uptake kinetics (K_1) which is an indicator of the transporters regulation. In fact K_1 value in glioma group differed from that found in the control group.

Kabalka and coworkers reported a clinical application of BNCT devoted to the treatment of metastatic malignant melanoma by means of ^{18}FBPA.[67] Their work dealt with a patient with widely metastatic malignant melanoma involving the torax and brain. The PET images clearly identified a brain lesion that was difficulty visualized by CT and MRI. The first case of a clinical application of BNCT to head and neck malignancy was reported on 2006.[68] The patient was a 48-year-old woman with recurrent submandibular gland cancer. The study confirmed the accumulating capacity of BPA in the tumor by the application of ^{18}F labeled BPA PET. The BNCT treatment caused a complete

regression of the tumor and no acute and chronic complications for 1.5 years. The results are showed in Figure 11 and Figure 12.
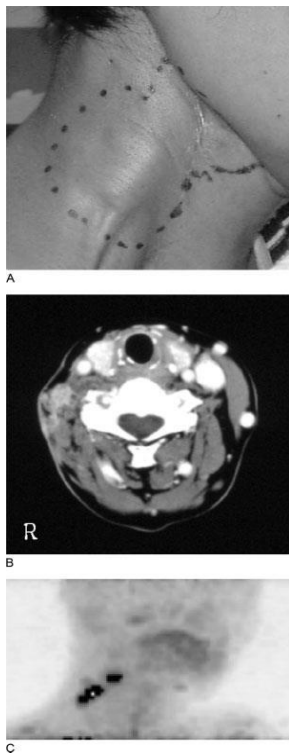

Figure 11 (A) Local findings before BNCT. (B) Neck CT before BNCT. (C) ^{18}F BPA PET examination where BPA uptake was measured (images reprinted with the permission of the editor, license number 2762421391809).
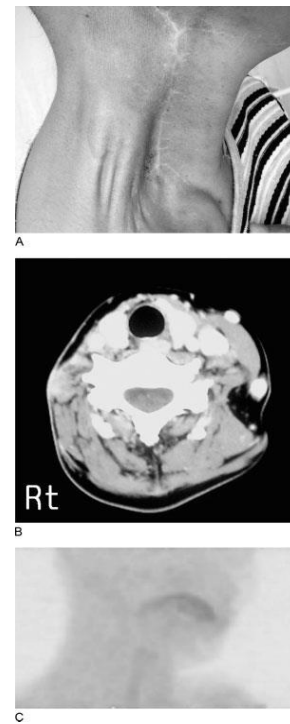
Figure 12 (A) Local appearance 12 months after BNCT. (B) The tumor region was cicatrized on CT performed 12 months after irradiation. (C) ^{18}F BPA PET performed 12 months after irradiation. No accumulation of BPA in lesion was noticed (images reprinted with the permission of the editor, license number 2762421391809).

Another PET/CT study dealt with a patient with a melanoma at the right ankle.[69] This study demonstrated that PET technique associated to computed tomography (CT) could give precise and regional indication on viable proliferating tissue. In the author opinion, it means that a more precise and well shaped ^{10}B mapping could be achieved and applied to a BNCT treatment. As shown in Figure 13 the tracer biodistribution was best appreciated in maximum intensity projection (MIP) images with bladder as a critical organ. The images were realized at the Turku PET centre, University of Turku, Finland.

Figure 13 Coronal [18]FBFA of a patient with melanoma in right ankle (not shown) metastatic to right inguinal lymph node (visible in all images) (images reprinted with the permission of the editor, license number 2762430074710).

SPECT Detection

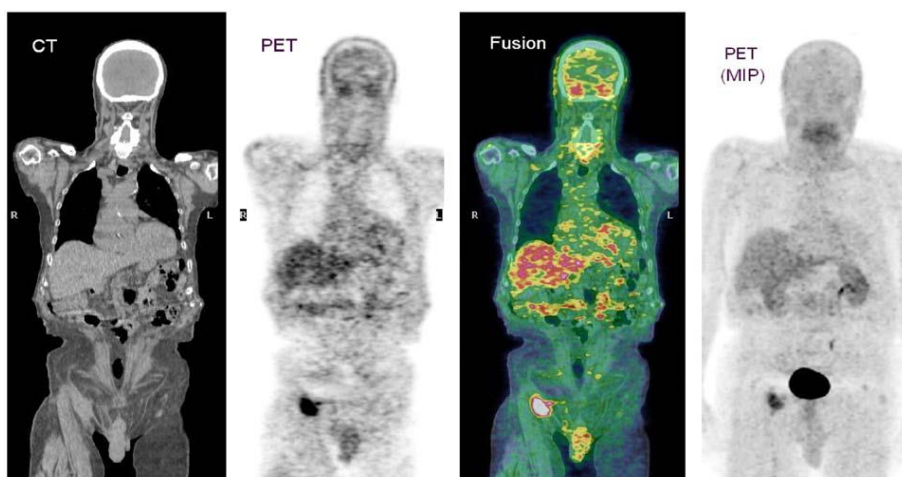Radionuclides that are useful for SPECT imaging emit photons in high abundance and have high enough energy (>100 Kev) to readily escape the body and be detected. The most common isotopes used in SPECT are [99m]Tc (t ½ =6h), [125]I (t ½ =59 days) and [131]I (t ½ =8 days).

Carborane clusters have been investigated intensively over the past decade as "prosthetic group" for radiohalogenation tumorseeking biomolecules for targeted radionuclide therapy, in order to overcome the undesired release of radiohalogen. One of the general problem associated with the use of radioiodinated compounds containing conventional C-I bonds is their susceptibility to dehalogenation, leading to an accumulation of radioactive material mostly in thyroid and stomach.[70] The B-I bond is substantially stronger than the C-I bond and consequently is more stable towards *in vivo* enzymatic and hydrolytic cleavage.[71]

Carborane cage iodination strategies were predominantly explored using the negatively-charged *nido*-carborane cluster because of its high reactivity towards electrophilic species.[72] One of the successful strategies was the attachment of *nido*-carborane to a vector molecule, which would carry it to the cellular target, followed by radioiodination of the resulting conjugate. IodoGen® (1,3,4,6-tetrachloro-3a,6a-diphenylglucuril) or Chloramine–T (sodium N –para-toluene solfonammide) were used to generate electrophilic iodine running the reaction in a slightly acid conditions.[73] Biomolecule vectors that have been employed include e.g. biotin,[74, 75] monoclonal antibodies (mAbs) and F(ab')2 fragments of mABs (Figure 14 a, b).[76]

The same reaction conditions can be employed to radiolabel other carborane cluster such as *closo*-monocarbon carborane, *nido*-monocarbon carborane and *closo*-decaborate. Scott Wilbur and coworkers have been investigating the *in vivo* stability and distribution properties of astatinated derivatives as reagents for carrying [211]At in cancer pretargeting protocols for a certain number of years. As a mean of increasing the *in vivo* stability of [211]At-labeled proteins they have been investigating antiboby conjugates of boron cage moieties in substitution of aryl conjugated. *Nido*-carboranes, bis-*nido*-carboranes and *closo*-decaborate have been prepared, the Venus Fly-Trap derivative (a bis-*nido*-carboranes compound) is depicted in Figure 14c.[73-75, 77, 78] In particular, their study have shown that the use of *closo*-decaborate moiety for [211]At-labeling of biomolecules provided high *in vivo* stability towards deastatination.[79] Wilbur and coworkers accomplished

14

radioiodination of several anionic *nido-* and *closo-*monocarbon carboranes.[80] by using the methodology reported for the inclusion of [211]At. *Nido-*monocarbon carboranes demonstrated to be more reactive than *closo-*monocarborn carboranes (Figure 14e). Moreover unsubstituted carboranes underwent iodination reaction more rapidly than substituted ones, thus they could be radioiodinated at a higher specific activity. These results supported their use in the development of compounds for BNCT. Biodistribution of ^{131}I and [125]I *nido-* and *closo-* carboranes were similar in mice, but blood clearance of the *nido-*derivatives was slower.

The *nido-*carborane cage has been also proposed as a pendant group for labelling proteins with [99m]Tc (Figure 14d). This metallocarborane cluster showed an extraordinary stability and could be readily prepared and conjugated.[81]

The radiohalogenation of *closo-*carboranes has also been studied, although not in the context of biomolecules.[82] *Closo-*carboranes require harsher electrophilic reaction conditions for halogenation in comparison to the *nido-*carboranes, using e.g. Lewis acids such AlCl$_3$ in combination with I$_2$ or NaI and long reaction times. Such conditions are not compatible with the use of radioctive isotopes that have shorter half-lives. Sjoeberg and Tolmachev proposed a new strategy for the radiohalogenation of *closo* -o-, m-, and p-carboranes, which employs coventional "cold" cluster iodination followed by Pd-catalyzed isotopic exchange.[83]
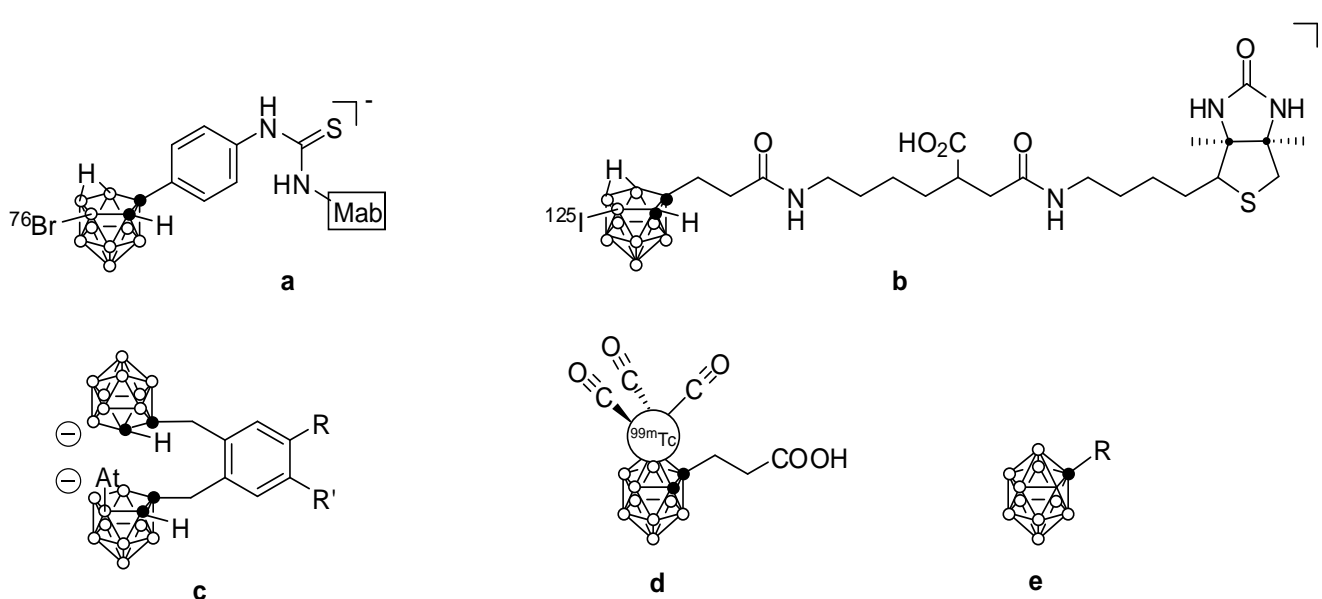
Figure 14 a) Radiobrominated nido-carborane conjugated to antibodies, **b**) radioiodinated boron-containing derivates of biotin, **c**) astatinated Venus Fly-Trap, **d**) ^{99m}Tc-labelled metallocarborane, **e**) *closo-*monocarbon carborane derivative.

Discussion.

Quantitative information regarding local [10]B concentration is crucial to determining the optimal timing of the neutron irradiation and to calculating the radiation dose. One of the problems confronting the successful clinical implementation of BNCT is the difficulty of quantitatively mapping the distribution of the boron containing molecules in patients during the treatment.[57-59] Furthermore, the clinical efficacy of the therapy is only guaranteed if the boron is located inside a tumor cell at a concentration of at least 20-30 ppm.

Currently, the concentrations of ^{10}B in tumor-cells are estimated using empirical data models that depend on tumor-to-blood, tumor-to-brain and brain-to- blood ^{10}B concentration ratios. One of the problems is that the uptake and distribution of ^{10}B varies among patients and that large uncertainties exist in the tumor-to-blood ^{10}B concentration ratio.[57, 58, 84]

At the same time the selective delivery of the NCT agent becomes one of the crucial points for the success of the treatment and only two compounds (BPA and BSH) have been extensively tested in both pre-clinical and clinical trials. Only proper NCT agent design, based on an improved knowledge of how molecules enter healthy and diseased cells, could allow the minimal intracellular concentration, needed to make NCT an effective therapy to cure cancer, to be reached. Furthermore, the recent development of non invasive and highly sensitive imaging techniques permits the detection of tumor boron concentration in real time before neutron treatment. Some of these methodologies require the functionalization of the NC agent with a proper imaging reporter, such as ^{18}F atoms for PET, a Gd/Fe containing agent for MRI or ^{19}F atoms for ^{19}F-NMR. Other spectroscopic methods do not require any NC agent modification (^{10}B NMR, MRS, MRSI), however their sensitivity is significantly lower and currently does not allow the quantification of the boron amount accumulated at the tumor site during standard BNCT protocols to be carried out. Furthermore, direct ^{10}B detection needs additional nonstandard hardware, usually not provided on clinical scanners. However, the continuous improvement and development of new specific sequences together with the use in clinic of more and more high magnetic fields (>3Tesla) will allow these techniques to reach the minimum boron threshold used during BNCT treatment. Both PET and MRI detection limits are under the boron threshold that has to be reached to perform this therapy but PET has the disadvantage of the administration of further radioactivity and needs to prepare a radioactively labeled NCT agent. MRI is safe but needs contrast agents with a molecular weight of around 600 Da. which contain residual charges that can dramatically change the biodistribution of the boron containing agent once conjugated. Furthermore, syntheses, purification and characterization of MRI contrast agents containing carborane is quite difficult since it needs a lot of steps and long reaction times. On the basis of these considerations it is possible to conclude that it is necessary to improve imaging protocols in order to measure boron concentration and provide images of the spatial distribution in target tumor cells. For PET and MRI this means to prepare and test more sensitive and specific probes, whereas for other spectroscopic methods to find more effective sequences and hardware components. The development of the imaging techniques described in this review is fundamental for the design and testing of new boron compounds with improved selectivity and the capability to carry higher boron payloads than those of the currently clinically approved BPA and BSH.

Acknowledgment

References

[1]   Barth, R. F., Boron neutron capture therapy at the crossroads: Challenges and opportunities. *Appl. Radiat. Isotopes* **2009,** 67, (7-8, Supplement 1), S3-S6.

[2]   Barth, R. F.; Coderre, J. A.; Vicente, M. G. H.; Blue, T. E., Boron Neutron Capture Therapy of Cancer: Current Status and Future Prospects. *Clin. Cancer Res.* **2005,** 11, (11), 3987-4002.

[3]   Mamelak, A. N.; Jacoby, D. B., Targeted delivery of antitumoral therapy to glioma and other malignancies with synthetic chlorotoxin (TM-601). *Expert Opinion on Drug Delivery* **2007,** 4, (2), 175-186.

[4]   Yan, H.; Parsons, D. W.; Jin, G.; McLendon, R.; Rasheed, B. A.; Yuan, W.; Kos, I.; Batinic-Haberle, I.; Jones, S. n.; Riggins, G. J.; Friedman, H.; Friedman, A.; Reardon, D.; Herndon, J.; Kinzler, K. W.; Velculescu, V. E.; Vogelstein, B.; Bigner, D. D., IDH1 and IDH2 Mutations in Gliomas. *N. Eng. J. Med.* **2009,** 360, (8), 765-773.

[5]   Macbeth, A. E.; Grindlay, D. J. C.; Williams, H. C., What's new in skin cancer? An analysis of guidelines and systematic reviews published in 2008-2009. *Clinical and Experimental Dermatology* **2011,** 36, (5), 453-458.

[6]   Gavriel, H.; McArthur, G.; Sizeland, A.; Henderson, M., Review: mucosal melanoma of the head and neck. *Melanoma Res.* **2011,** 21, (4), 257-266.

[7]   Andersen, K. F.; Altaf, R.; Krarup-Hansen, A.; Kromann-Andersen, B.; Horn, T.; Christensen, N. J.; Hendel, H. W., Malignant pheochromocytomas and paragangliomas - The importance of a multidisciplinary approach. *Cancer Treatment Reviews* **2011,** 37, (2), 111-119.

[8]   Livraghi, T.; Makisalo, H.; Line, P. D., Treatment options in hepatocellular carcinoma today. *Scandinavian Journal of Surgery* **2011,** 100, (1), 22-29.

[9]   Clifton, N.; Harrison, L.; Bradley, P. J.; Jones, N. S., Malignant melanoma of nasal cavity and paranasal sinuses: report of 24 patients and literature review. *Journal of Laryngology & Otology* **2011,** 125, (5), 479-485.

[10]   Tawfik, A. M.; Kreft, A.; Wagner, W.; Vogl, T. J., MRI of a microcystic adnexal carcinoma of the skin mimicking a fibrous tumour: case report and literature review. *Br. J. Radiol.* **2011,** 84, (1002), E114-E117.

[11]   De la Fouchardiere, C.; Droz, J. P., Targeted therapies and thyroid cancer: an update. *Anti-Cancer Drugs* **2011,** 22, (7), 688-699.

[12]   Ferraz, C.; Eszlinger, M.; Paschke, R., Current State and Future Perspective of Molecular Diagnosis of Fine-Needle Aspiration Biopsy of Thyroid Nodules. *J. Clin. Endocrinol. Metab.* **2011,** 96, (7), 2016-2026.

[13]   Snider, H. R.; Reedy, A. J.; Lennarz, W. J., Synthesis of aromatic boronic acids, aldehydo boronic acids and a boronic acids analog of tyronise. *J. Am. Chem. Soc.* **1958,** 80, 835-838.

[14]   Soloway, A. H.; Hatanaka, H.; Davis, M. A., Penetration of brain and brain tumor. VII. Tumor-binding sulphydryl boron compounds. *J. Med. Chem.* **1967,** 10, (714-717).

[15]   Hatanaka, H. A., Revised boron-neutron capture therapy for malignant brain tumors: II. Interim clinical result with patients excluding previous treatment. *J. Neurol.* **1975,** 209, 81-94.

[16]   Mishima, Y.; Honda, C.; Ichihashi, M.; Obara, H.; Hiratsuka, J.; Fukuda, H.; Karashima, H.; Kobayashi, T.; Kanda, K.; Yoshino, K., Treatment of malignant melanoma by single thermal neutron capture therapy with melanoma-seeking 10B compound. *The Lancet* **1989,** 334, (8659), 388-389.

[17]   Diaz, A. Z., Assessment of the results from the phase I/II boron neutron capture therapy trials at the Brookhaven National Laboratory from a clinician's point of view. *J. Neurooncol.* **2003,** 62, (1), 101-109.

[18]   Ichikawa, H.; Taniguchi, E.; Fujimoto, T.; Fukumori, Y., Biodistribution of BPA and BSH after single, repeated and simultaneous administrations for neutron-capture therapy of cancer. *Appl. Radiat. Isotopes* **2009,** 67, (7-8), S111-S114.

[19]   Yokoyama, K.; Miyatake, S. I.; Kajimoto, Y.; Kawabata, S.; Doi, A.; Yoshida, T.; Asano, T.; Kirihata, M.; Ono, K.; Kuroiwa, T., Pharmacokinetic study of BSH and BPA in simultaneous use for BNCT. *J. Neurooncol.* **2006,** 78, (3), 227-232.

17

[20]   Valliant, J. F.; Guenther, K. J.; King, A. S.; Morel, P.; Schaffer, P.; Sogbein, O. O.; Stephenson, K. A., The medicinal chemistry of carboranes. *Coord. Chem. Rev.* **2002,** 232, (1-2), 173-230.

[21]   Wu, G.; Barth, R. F.; Yang, W.; Lee, R. J.; Tjarks, W.; Backer, M. V.; Backer, J. M., Boron Containing Macromolecules and Nanovehicles as Delivery Agents for Neutron Capture Therapy. *Anti Cancer Agents in Medicinal Chemistry* **2006,** 6, 167-184.

[22]   Crossley, E. L.; Ziolkowski, E. J.; Coderre, J. A.; Rendina, L. M., Boronated DNA-Binding Compounds as Potential Agents for Boron Neutron Capture Therapy. *Mini reviews in Medicinal Chemistry* **2007,** 7, 303-313.

[23]   Sweet, W. H., The use of nuclear desintegrations in the diagnosis and treatment of brain tumor. *N. Engl. J. Med.* **1951,** 245, 875-878.

[24]   RF. Barth, J. C., MGH. Vincente, TE. Blue, , Boron Neutron Capture Therapy of Cancer: Current Status and Future Prospects. *Clin. Cancer. Res.* **2005,** 11, 3987-4001.

[25]   Ruiz-Cabello, J.; Barnett, B. P.; Bottomley, P. A.; Bulte, J. W. M., Fluorine ((19)F) MRS and MRI in biomedicine. *Nmr Biomed.* **2011,** 24, (2), 114-129.

[26]   Hattori, Y.; Asano, T.; Niki, Y.; Kondoh, H.; Kirihata, M.; Yamaguchi, Y.; Wakamiya, T., Study on the compounds containing 19F and 10B atoms in a single molecule for the application to MRI and BNCT. *Bioorg. Med. Chem.* **2006,** 14, (10), 3258-3262.

[27]   Hattori, Y.; Yamamoto, H.; Ando, H.; Kondoh, H.; Asano, T.; Kirihata, M.; Yamaguchi, Y.; Wakamiya, T., Synthesis and evaluation as MRI probe of the trifluoromethylated p-boronophenylalanine and its alcohol derivative. *Bioorg. Med. Chem.* **2007,** 15, (5), 2198-2205.

[28]   Hattori, Y.; Kurihara, K.; Kondoh, H.; Asano, T.; Kirihata, M.; Yamaguchi, Y.; Wakamiya, T., Biological evaluation of fluorinated p-boronophenylalanine derivatives as a boron carrier. *Protein Pept. Lett.* **2007,** 14, (3), 269-272.

[29]   Capuani, S.; Porcari, P.; Fasano, F.; Campanella, R.; Maraviglia, B., 10B-editing 1H-detection and 19F MRI strategies to optimize boron neutron capture therapy. *Magn. Reson. Imaging* **2008,** 26, (7), 987-993.

[30]   Porcari, P.; Capuani, S.; Campanella, R.; La Bella, A.; Migneco, L. M.; Maraviglia, B., Multi-nuclear MRS and F-19 MRI of F-19-labelled and B-10-enriched p-boronophenylalanine-fructose complex to optimize boron neutron capture therapy: phantom studies at high magnetic fields. *Phys. Med. Biol.* **2006,** 51, (12), 3141-3154.

[31]   Capuani, S.; Gili, T.; Bozzali, M.; Russo, S.; Porcari, P.; Cametti, C.; Muolo, M.; D'Amore, E.; Maraviglia, B.; Lazzarino, G.; Pastore, F. S., Boronophenylalanine uptake in C6 glioma model is dramatically increased by L-DOPA preloading. *Appl. Radiat. Isotopes* **2009,** 67, (7-8, Supplement 1), S34-S36.

[32]   Porcari, P.; Capuani, S.; D'Amore, E.; Lecce, M.; La Bella, A.; Fasano, F.; Campanella, R.; Migneco, L. M.; Pastore, F. S.; Maraviglia, B., In Vivo F-19 MRI and F-19 MRS of F-19-labelled borophenylalanine-fructose complex on a C6 rat glioma model to optimize boron neutron capture therapy (BNCT). *Phys. Med. Biol.* **2008,** 53, (23), 6979-6989.

[33]   Porcari, P.; Capuani, S.; D'Amore, E.; Lecce, M.; La Bella, A.; Fasano, F.; Migneco, L. M.; Campanella, R.; Maraviglia, B.; Pastore, F. S., In vivo 19F MR imaging and spectroscopy for the BNCT optimization. *Appl. Radiat. Isotopes* **2009,** 67, (7-8, Supplement 1), S365-S368.

[34]   Chen, B.-G.; Zhang, M.-Y.; Zhao, Y.-Y.; Zhang, J.; Sun, C.-C., Structural and electronic properties of BPA-fructose complex used in boron neutron capture therapy. *Journal of Molecular Structure: THEOCHEM* **2006,** 766, (1), 35-40.

[35]   Bendel, P.; Koudinova, N.; Salomon, Y., In vivo imaging of the neutron capture therapy agent BSH in mice using 10B MRI. *Magn. Res. Med.* **2001,** 46, (1), 13-17.

[36]   Elhanati, G.; Salomon, Y.; Bendel, P., Significant differences in the retention of the borocaptate monomer (BSH) and dimer (BSSB) in malignant cells. *Cancer Lett.* **2001,** 172, (2), 127-132.

18

[37]   Bendel, P.; Wittig, A.; Basilico, F.; Mauri, P. L.; Sauerwein, W., Metabolism of borono-phenylalanine-fructose complex (BPA-fr) and borocaptate sodium (BSH) in cancer patients--Results from EORTC trial 11001. *J. Pharm. Biomed. Anal.*   **2010,** 51, (1), 284-287.

[38]   Rinck, A., *Magnetic Resonance in Medicine*. Blackwell Scientific Publications: Oxford, 2003.

[39]   Terreno , E.; Castelli, D. D.; Viale , A.; Aime, S., Challenges for molecular magnetic resonance imaging. *Chem. Rev.* **2010,** 110, (5), 3019-3042.

[40]   Caravan, P., Strategies for increasing the sensitivity of gadolinium based MRI contrast agents. *Chem. Soc. Rev.* **2006,** 35, (6), 512-23.

[41]   Aime , S.; Cabella , C.; Colombatto , S.; Geninatti-Crich , S.; Gianolio , E.; Maggioni, F., Insights into the use of paramagnetic Gd(III) complexes in MR-molecular imaging investigations. *J. Magn. Reson. Imaging* **2002,** 16, 394-406.

[42]   Tatham , A. T.; Nakamura , H.; Wiener , E. C.; Yamamoto, Y., Relaxation properties of a dual-labeled probe for MRI and neutron capture therapy. *Magn. Reson. Med.* **1999,** 42, 32-6.

[43]   Takahashi , K.; Nakamura , H.; Furumoto , S.; Yamamoto , K.; Fukuda , H.; Matsumura , A.; Yamamoto, Y., Synthesis and in vivo biodistribution of BPA-Gd-DTPA complex as a potential MRI contrast carrier for neutron capture therapy. *Bioorg. Med. Chem.* **2005,** 13, 735-43.

[44]   Nakamura , H.; Fukuda , H.; Girald , F.; Kobayashi, T.; Hiratsuka , J.; Akaizawa , T.; Nemoto , H.; Cai , J.; Yoshida , K.; Y., Y., In vivo evaluation of carborane gadolinium-DTPA complex as an MR imaging boron carrier. *Chem. Pharm. Bull.* **2000,** 48, 1034-8.

[45]   Geninatti-Crich, S.; Alberti, D.; Szabo, I.; Deagostino, A.; Toppino, A.; Barge, A.; Ballarini, F.; Bortolussi, S.; Bruschi, P.; Protti, N.; Stella, S.; Altieri, S.; Venturello, P.; Aime, S., MRI-guided neutron capture therapy by use of a dual gadolinium/boron agent targeted at tumour cells through upregulated low-density lipoprotein transporters. *Chem.--Eur. J.*   **2011,** 17, 8479-86.

[46]   Aime, S.; Barge, A.; Crivello, A.; Deagostino, A.; Gobetto, R.; Nervi, C.; Prandi, C.; Toppino, A.; Venturello, P., Synthesis of Gd(III)-C-palmitamidomethyl-C'-DOTAMA-C(6)-o-carborane: a new dual agent for innovative MRI/BNCT applications. *Org. Biomol. Chem.* **2008,** 6, 4460-6.

[47]   Golberg, D., Bando,Y.,Tang,C.,Zhi,C, Boronnitridenanotubes. *Adv.Mater.* **2007,** 19, 2413–2432.

[48]   Ciofani, G.; Raffa, V.; Menciassi, A.; Cuschieri, A., Folate functionalized boron nitride nanotubes and their selective uptake by glioblastoma multiforme cells: implications for their use as boron carriers in clinical boron neutron capture
therapy. *Nanoscale Res. Lett.* **2009,** 4, 113–121.

[49]   Menichetti, L.; DeMarchi, D.; Calucci, L.; Ciofani, G.; Menciassi, A.; Forte, C., Boron nitride nanotubes for boron neutron capture therapy as contrast agents in magnetic resonance imaging a t3T. *Appl. Radiat. Isotopes* **2011,** 25, in press.

[50]   Calucci, L.; Ciofani, G.; DeMarchi, D.; Forte, C.; Menciassi, A.; Menichetti, L.; Positano, V., Boron Nitride Nanotubes as T-2-Weighted MRI Contrast Agents. *J. Phys. Chem. Lett* **2010,** 1, 2561-2565.

[51]   Isobe, T.; Matsumura, A.; Anno, I.; Yoshizawa, T.; Nagatomo, Y.; Itai, Y.; Nose, T., Quantification of cerebral metabolites in glioma patients with proton MR spectroscopy using T2 relaxation time correction. *Magn. Reson. Imaging* **2002,** 20, (4), 343-349.

[52]   Yamamoto, Y.; Isobe, T.; Yamamoto, T.; Shibata, Y.; Anno, I.; Nakai, K.; Shirakawa, M.; Matsushita, A.; Sato, E.; Matsumura, A., T2 corrected quantification method of L-p-boronophenylalanine using proton magnetic resonance spectroscopy for boron neutron capture therapy. *Appl. Radiat. Isotopes* **2009,** 67, S345–S347.

[53]   Heikkinen, S.; Kangasmaki, A.; Timonen, M.; Kankaanranta, L.; Hakkinen, A.; Lundborn, N.; Vahatalo, J.; Savolainen, S., H-1 MRS of a Boron Neutron Capture Therapy B-10 Carrier, L-p-boronophenylalanine-fructose complex, BPA-F: phantom studies at 1.5 and 3.0 T. *Phys. Med. Biol.* **2003,** 48, (8), 1027-1039.

19

[54]   Bendel, P.; Sauerwein, W., Optimal detection of the neutron capture therapy agent borocaptate sodium (BSH): A comparison between [sup 1]H and [sup 10]B NMR. *Med. Phys.* **2001,** 28, (2), 178-183.

[55]   Timonen, M.; Kankaanranta, L.; Lundbom, N.; Collan, J.; Kangasmäki, A.; Kortesniemi, M.; Häkkinen, A. M.; Lönngren, A.; Karjalainen, S.; Rasilainen, M.; Leinonen, J.; Huitti, T.; Jääskeläinen, J.; Kouri, M.; Savolainen, S.; Heikkinen, S., 1H MRS studies in the Finnish boron neutron capture therapy project: Detection of 10B-carrier, l-p-boronophenylalanine-fructose. *Eur. J. Radiol.* **2005,** 56, (2), 154-159.

[56]   Zuo, C. S.; Prasad, P. V.; Busse, P.; Tang, L.; Zamenhof, R. G., Proton nuclear magnetic resonance measurement of p-boronophenylalanine (BPA): A therapeutic agent for boron neutron capture therapy. *Med. Phys.* **1999,** 26, (7), 1230-1236.

[57]   Bendel, P.; Margalit, R.; Salomon, Y., Optimized 1H MRS and MRSI methods for the in vivo detection of boronophenylalanine. *Magn. Res. Med.* **2005,** 53, (5), 1166-1171.

[58]   Timonen, M.; Kangasmaki, A.; Savolainen, S.; Heikkinen, S., H-1 MRS phantom studies of BNCT B-10-carrier, BPA-F using STEAM and PRESS MRS sequences: Detection limit and quantification. *Spectroscopy* **2004,** 18, (2), 133-142.

[59]   Wittig, A.; Michel, J.; Moss, R. L.; Stecher-Rasmussen, F.; Arlinghaus, H. F.; Bendel, P.; Mauri, P. L.; Altieri, S.; Hilger, R.; Salvadori, P. A.; Menichetti, L.; Zamenhof, R.; Sauerwein, W. A. G., Boron analysis and boron imaging in biological materials for Boron Neutron Capture Therapy (BNCT). *Crit. Rev. Onc. Hemat.* **2008,** 68, (1), 66-90.

[60]   Adam, M. J.; Wilbur, D. S., Radiohalogens for imaging and therapy. *Chem. Soc. Rev.* **2005,** 34, (2), 153-163.

[61]   Kabalka, G. W.; Smith, G. T.; Dyke, J. P.; Reid, W. S.; Longford, C. P. D.; Roberts, T. G.; Reddy, N. K.; Buonocore, E.; Hubner, K. F., Evaluation of fluorine-18-BPA-fructose for boron neutron capture treatment planning. *Journal of Nuclear Medicine* **1997,** 38, (11), 1762-1767.

[62]   Imahori, Y.; Ueda, S.; Ohmori, Y.; Kusuki, T.; Ono, K.; Fujii, R.; Ido, T., Fluorine-18-labeled fluoroboronophenylalanine PET in patients with glioma. *Journal of Nuclear Medicine* **1998,** 39, (2), 325-333.

[63]   Imahori, Y.; Ueda, S.; Ohmori, Y.; Sakae, K.; Kusuki, T.; Kobayashi, T.; Takagaki, M.; Ono, K.; Ido, T.; Fujii, R., Positron emission tomography-based boron neutron capture therapy using boronophenylalanine for high-grade gliomas: Part II. *Clinical Cancer Research* **1998,** 4, (8), 1833-1841.

[64]   Takahashi, Y.; Imahori, Y.; Mineura, K., Prognostic and therapeutic indicator of fluoroboronophenylalanine positron emission tomography in patients with gliomas. *Clin. Cancer Res.* **2003,** 9, (16), 5888-5895.

[65]   Chen, J. C.; Chang, S. M.; Hsu, F. Y.; Wang, H. E.; Liu, R. S., MicroPET-based pharmacokinetic analysis of the radiolabeled boron compound [F-18]FBPA-F in rats with F98 glioma. *Appl. Radiat. Isotopes* **2004,** 61, (5), 887-891.

[66]   Wang, H. E.; Liao, A. H.; Deng, W. P.; Chang, P. F.; Chen, J. C.; Chen, F. D.; Liu, R. S.; Lee, J. S.; Hwang, J. J., Evaluation of 4-borono-2-F-18-fluoro-L-phenylalanine-fructose as a probe for boron neutron capture therapy in a glioma-bearing rat model. *J. Nucl. Med.* **2004,** 45, (2), 302-308.

[67]   Kabalka, G. W.; Nichols, T. L.; Smith, G. T.; Miller, L. F.; Khan, M. K.; Busse, P. M., The Use of Positron Emission Tomography to Develop Boron Neutron Capture Therapy Treatment Plans for Metastatic Malignant Melanoma. *Journal of Neuro-Oncology* **2003,** 62, (1), 187-195.

[68]   Aihara, T.; Hiratsuka, J.; Morita, N.; Uno, M.; Sakurai, Y.; Maruhashi, A.; Ono, K.; Harada, T., First clinical case of boron neutron capture therapy for head and neck malignancies using F-18-BPA pet. *Head & Neck* **2006,** 28, (9), 850-855.

[69]   Menichetti, L.; Cionini, L.; Sauerwein, W. A.; Altieri, S.; Solin, O.; Minn, H.; Salvadori, P. A., Positron emission tomography and [(18)F]BPA: A perspective application to assess tumour extraction of boron in BNCT. *Applied Radiation and Isotopes* **2009,** 67, (7-8), S351-S354.

[70]   Hawthorne, M. F.; Maderna, A., Applications of radiolabeled boron clusters to the diagnosis and treatment of cancer. *Chem. Rev.* **1999,** 99, (12), 3421-3434.

[71]   Armstrong, A. F.; Valliant, J. F., The bioinorganic and medicinal chemistry of carboranes: from new drug discovery to molecular imaging and therapy. *Dalton Trans.* **2007**, 4240-4251.

[72]   Varadarajan, A.; Sharkey, R. M.; Goldenberg, D. M.; Hawthorne, M. F., Conjugation of Phenyl Isothiocyanate Derivatives of Carborane to Antitumor Antibody and Invivo Localization of Conjugates in Nude-Mice. *Bioconjugate Chem.* **1991,** 2, (2), 102-110.

[73]   Wilbur, D. S.; Hamlin, D. K.; Livesey, J. C.; Srivastava, R. R.; Laramore, G. E.; Griffin, T. W., *Nucl. Med. Biol.* **1994,** 21, 601-611.

[74]   Wilbur, D. S.; Chyan, M. K.; Hamlin, D. K.; Perry, M. A., Reagents for Astatation of Biomolecules. 3. Comparison of closo-Decaborate(2-) and closo-Dodecaborate(2-) Moieties as Reactive Groups for Labeling with Astatine-211. *Bioconjugate Chem.* **2009,** 20, (3), 591-602.

[75]   Wilbur, D. S.; Hamlin, D. K.; Chyan, M. K.; Kegley, B. B.; Quinn, J.; Vessella, R. L., Biotin reagents in antibody pretargeting. 6. Synthesis and in vivo evaluation of astatinated and radioiodinated aryl- and nido-carboranyl-biotin derivatives. *Bioconjugate Chem.* **2004,** 15, (3), 601-616.

[76]   Wilbur, D. S.; Hamlin, D. K.; Chyan, M. K.; Brechbiel, M. W., Streptavidin in antibody pretargeting. 5. Chemical modification of recombinant streptavidin for labeling with the alpha-particle-emitting radionuclides Bi-213 and At-211. *Bioconjugate Chem.* **2008,** 19, (1), 158-170.

[77]   Wilbur, D. S.; Chyan, M. K.; Hamlin, D. K.; Vessella, R. L.; Wedge, T. J.; Hawthorne, M. F., Reagents for astatination of biomolecules. 2. Conjugation of anionic boron cage pendant groups to a protein provides a method for direct labeling that is stable to in vivo deastatination. *Bioconjugate Chem.* **2007,** 18, (4), 1226-1240.

[78]   Wilbur, D. S.; Thakar, M. S.; Hamlin, D. K.; Santos, E. B.; Chyan, M. K.; Nakamae, H.; Pagel, J. M.; Press, O. W.; Sandmaier, B. M., Reagents for Astatation of Biomolecules. 4. Comparison of Maleimido-closo-Decaborate(2-) and meta-[(211)At]Astatobenzoate Conjugates for Labeling anti-CD45 Antibodies with [(211)At]Astatine. *Bioconjugate Chem.* **2009,** 20, (10), 1983-1991.

[79]   Wilbur, D. S.; Chyan, M.-K.; Hamlin, D. K.; Perry, M. A., Preparation and in vivo evaluation of radioiodinated closo-decaborate (2-) derivatives to identify structural components that provide low retention in tissues. *Nucl. Med. Biol.*   **2010,** 37, (2), 167-178.

[80]   Wilbur, D. S.; Hamlin, D. K.; Srivastava, R. R.; Chyan, M. K., Synthesis, radioiodination, and biodistribution of some nido- and closo-monocarbon carborane derivatives. *Nucl. Med. Biol.* **2004,** 31, (4), 523-530.

[81]   Sogbein, O. O.; Merdy, P.; Morel, P.; Valliant, J. F., Preparation of Re(I)-and Tc99m(I)-metallocarboranes in Water under Weakly Basic Reaction Conditions. *Inorg. Chem.* **2004,** 43, (10), 3032-3034.

[82]   Eriksson, L.; Tolmachev, V.; Sjoberg, S., Feasibility of palladium-catalyzed isotopic exchange between sodium [I-125]I and 2-iodo-para-carborane. *J. Labelled Compd. Radiopharm.* **2003,** 46, (7), 623-631.

[83]   Winberg, K. J.; Barbera, G.; Eriksson, L. B.; Teixidor, F.; Tolmachev, V.; Vinas, C.; Sjoberg, S., High yield [I-125]iodide-labeling of iodinated carboranes by palladium-catalyzed isotopic exchange. *J. Organomet. Chem.*   **2003,** 680, (1-2), 188-192.

[84]   Laakso, J.; Kulvik, M.; Ruokonen, I.; Vähätalo, J.; Zilliacus, R.; Färkkilä, M.; Kallio, M., Atomic emission method for total boron in blood during neutron-capture therapy. *Clin. Chem.* **2001,** 47, 1796–1803.

21